International Journal of Mass Spectrometry 299 (2011) 5–8

Contents lists available at ScienceDirect

International Journal of Mass Spectrometry

journal homepage: www.elsevier.com/locate/ijms

Time-of-flight mass spectroscopy of femtosecond and nanosecond laser ablated TeO_2 crystals

S. Beke[a,*], T. Kobayashi[a], K. Sugioka[a], K. Midorikawa[a], J. Bonse[b]

[a] Laser Technology Laboratory, RIKEN – Advanced Science Institute, Hirosawa 2-1, Wako, Saitama 351-0198, Japan
[b] BAM Federal Institute for Materials Research and Testing, Unter den Eichen 87, 12205 Berlin, Germany

ARTICLE INFO

Article history:
Received 10 June 2010
Received in revised form 24 August 2010
Accepted 24 August 2010
Available online 6 September 2010

Keywords:
Time-of-flight mass spectroscopy
Tellurium dioxide crystals
Femtosecond laser
Nanosecond laser
Ablation

ABSTRACT

Single-pulse femtosecond (fs) (pulse duration ~200 fs, wavelength 398 nm) and nanosecond (ns) (pulse duration 4 ns, wavelength 355 nm) laser ablation have been applied in combination with time-of-flight mass spectrometer (TOFMS) to analyze the elemental composition of the plasma plume of single-crystalline telluria (c-TeO_2, grown by the balance controlled Czochralski growth method). Due to the three-order difference of the peak intensities of the ns and fs-laser pulses, significant differences were observed regarding the laser-induced species in the plasma plume. Positive singly, doubly and triply charged Te ions (Te^+, Te_2^+, Te_3^+) in the form of their isotopes were observed in case of both irradiations. In case of the ns-laser ablation the TeO^+ formation was negligible compared to the fs case and there was no Te trimer (Te_3^+) formation observed. It was found that the amplitude of Te ion signals strongly depended on the applied laser pulse energy. Singly charged oxygen ions (O^+) are always present as a byproduct in both kinds of laser ablation.

1. Introduction

Tellurium dioxide crystal (TeO_2) is a transparent insulator, which is used in acousto-optical devices (beam deflectors, light modulators, tunable optical filters). This material features high optical homogeneity, low optical absorption and scattering, high optical power capability and high optical damage resistance [1,2]. TeO_2 has high refractive indices and it transmits in the mid-infrared part of the electromagnetic spectrum; hence, it is of technological interest for optical devices. Our previous studies have revealed that femtosecond (fs) laser ablation has a great potential for the surface microprocessing of single-crystalline (c-TeO_2) TeO_2 [3,4]. In the dynamics and mechanism of fs-laser ablation of TeO_2, however, there are still many open questions. For a more detailed understanding of the mechanism, an in situ study is indispensable. Using time-of-flight mass spectrometry (TOFMS) one can analyze the intensity ratios of different ionic species generated in the ablated plasma precisely, reproducibly and accurately [5]. In fact, TOFMS has been widely applied for laser ablation studies of various materials [6–12] so far, but never for TeO_2 to the best of our knowledge.

Here we take benefit of the excellent (single-pulse) sensitivity of our reflectron TOFMS setup in order to study the ionic species produced by the laser ablation with fs- and ns-laser pulses of similar laser wavelengths and focusing conditions throughout a wide range of mass-to-charge ratios. This process provides a universal detection method of ions over a wide mass range. In this paper, we use this system to investigate in situ the fs-laser ablation of TeO_2 in comparison with ns-laser ablation.

2. Experimental

2.1. Crystal growth procedure and sample preparation

Single-crystals of paratellurite (TeO_2) were grown by using the balance controlled Czochralski method. The description of the growth apparatus is given in Ref. [13]. For the crystal growth, a resistance furnace was employed in order to maintain low thermal gradients and minimize the eventual temperature fluctuation during the growth and post-growth processes. The crystals were grown from 6N pure TeO_2. Single-crystals were pulled along the ⟨1 1 0⟩ direction in sizes up to 50 mm in diameter and 50 mm in length. The seed rotation rate varied between 15 and 20 rounds per minute and the pulling rate was 0.8–1 mm/h. For the measurements samples were cut with a diamond saw and X-ray oriented with a precision better than 0.5°. Polished (1 1 0) TeO_2 surfaces were prepared by a standard method using SiC for grinding and AB Alpha Alumina (Buehler Linde A 0.3 μm) for mechanical polishing [3,13]. Paratellurite crystals have a band gap energy of 4.05 eV. Hence, we assume 2-photon absorption processes (as the single photon energies are 3.1 eV and 3.5 eV for the two relevant wavelengths of 398 nm and

* Corresponding author.
E-mail addresses: beke@riken.jp, beke@scientist.com (S. Beke).

1387-3806/$ – see front matter © 2010 Elsevier B.V. All rights reserved.
doi:10.1016/j.ijms.2010.08.022

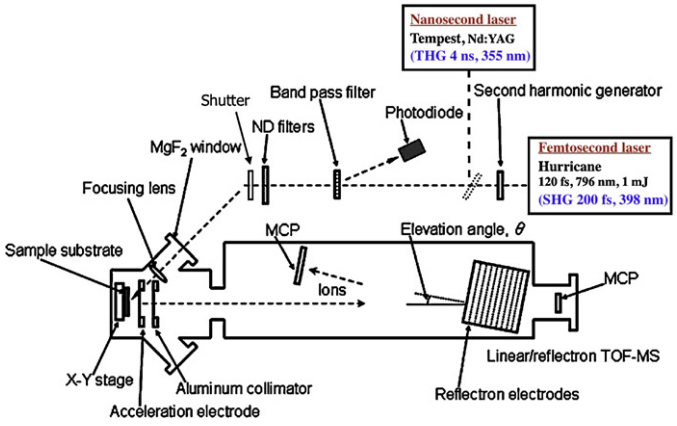

Fig. 1. Schematic of the TOFMS set up for the fs and ns ablation.

355 nm used in this study). In fact, impurities and crystal defects can cause local changes in the band structure with additional allowed energy levels in the band gap. For instance, oxygen vacancies may result in electron-donor states below the valence band [14]. Please note, that ablative removal of the thin gold layer from the surface prior to the experiments (see Section 2.2) could also cause various types of changes in the TeO_2 crystal (by unintentional irradiation of TeO_2) such as charged oxygen vacancies and non-bridging oxygen hole centers, which contribute to the appearance of new energy levels in the forbidden gap [15].

2.2. Time-of-flight analysis and laser processing of c-TeO_2

Fig. 1 shows the schematic of the experimental setup used for the TOFMS experiments allowing the use of different laser sources. Femtosecond laser pulses were supplied from a Ti:Sapphire laser system (Hurricane; Spectra-Physics) operating at 500 Hz repetition rate. The wavelength of the laser pulse was 796 nm with 120 fs pulse duration. The laser pulses were frequency-doubled using a 1 mm thick second harmonic generation crystal (BiBO crystal) resulting in a 398 nm femtosecond laser pulse of ~200 fs duration. A band-pass filter (03FCG033; Melles Griot, transparent to the 398 nm wavelength) was placed to suppress the non-converted fraction of the NIR fs-laser pulses. The filter was used only in the fs-laser irradiation experiments.

The typical fs pulse energy of 115 μJ after passing through the band-pass filter was adjusted in the 0.1–7.3 μJ range by passing through attenuating neutral density (ND) filters placed in front of a view port of the TOF vacuum chamber. A fast-response electromechanical shutter (Uniblitz LS6; Vincent Associates) was placed in the beam path to perform single-pulse measurements. The laser pulses were then focused by an achromatic lens of 70 mm focal length onto the sample surface at an incident angle of 45°. The laser spot diameter ($1/e^2$) was approx. 20 μm at the sample surface in the short direction of the elliptical spot. The 2 mm thick c-TeO_2 sample was mounted on an XY-translation stage and was moved by 150 μm after each irradiation (data acquisition) event. The laser pulse ablation was carried out under high vacuum conditions of 10^{-7} Torr.

The TOFMS was operated in a reflectron mode. In this mode, positive ions are accelerated by an external electric field in a direction normal to the sample substrate. The maximum voltage applied to the sample mount was +5 kV. A cathode mesh was placed at a distance of 6 mm from the sample and kept at 0 V. Ions traveling from the center of the flight path were blocked by an aluminum collimator with a hole (6 mm diameter). The accelerated ions were reflected from a potential gradient formed by reflection electrodes (elevation angle $\theta = 3.5°$). The termination voltage was +6 kV. Those ions were temporally separated by their mass-to-charge ratios during their flights and were detected using a three-stage MCP. The total flight path length was 1.7 m. Output signals from the MCP were recorded with a digital oscilloscope (WaveRunner 6050; LeCroy Corp.) through a fast preamplifier (model 9305; Ortec). The TOF measurements were synchronized to the laser pulse irradiation by means of a photodiode signal triggered from a part of the optical pulse reflected at the band-pass filter. The data of each individually recorded spectrum were smoothened by adjacent averaging over 20 data points to reduce the noise from the MCP detector.

In some complementary experiments, in order to compare with the results obtained by the fs laser, a nanosecond laser (New Wave Research "Tempest", Third Harmonic Generation (THG) of a Nd:YAG laser: 355 nm wavelength, 4 ns pulse duration) beam was passing through almost the same beam path as the fs-laser pulses just by placing a steering mirror into the setup and by replacing the band-pass filter. Care was taken to realize a similar laser spot diameter on the sample surface as in the fs-case. In this case, the wavelength of ns laser is close to that of fs laser, while the peak intensity is significantly different by the order of three, which should produce different specific species in the ablation plume.

Since electrical charging of the surface critically affects the proper acquisition of TOFMS spectra, prior to the laser irradiation experiments the c-TeO_2 samples were sputter-coated by a thin conductive layer of gold (~20 nm thickness). Therefore, a pre-irradiation sequence of 5–10 laser pulses per spot was required to locally remove the gold film and prepare a clean TeO_2 surface. This film removal was monitored *in situ* during the TOFMS experiment by tracking the Au^+ peak until it vanished almost completely. However, in some spectra it still can be noticed at 32 μs time of flight.

The experimentally measured times of flight have been used to identify the different positively charged ionic species which are generated during laser ablation and which are passing through the TOFMS without recombination. Based on the energy balance of ions being accelerated in an external electric field, the time of flight (TOF) can be calculated according to $TOF = k\sqrt{m/q}$, with m and q being the mass and the charge of the ions, respectively. The proportionality constant k includes experimental factors related to the instrument settings and characteristics. Once k is known from a calibration, the latter equation can be used to extract the mass-to-charge ratio directly from the TOF. The maximum mass resolution of the TOFMS under the given conditions was estimated to be $m/\Delta m$ ~300.

3. Results and discussion

3.1. Femtosecond laser ablation

Fig. 2 shows typical TOFMS spectrum, recorded upon ablation of TeO_2 by the single fs-laser pulse at a laser pulse energy of 3.0 μJ (fluence 1.0 J cm^{-2}, peak intensity 6.4×10^{12} W cm^{-2}). For the better visibility of the peaks, the spectrum is divided into three different temporal ranges (a: 0–20 μs, b: 20–30 μs, c: 30–45 μs). The peaks between 2 and 10 μs [Fig. 2(a)] are attributed to light elements such as H^+, C^+ and O^+ arriving the earliest at the detector. At 13.1 μs, 15.1 μs and 17 μs, the O_2^+, Te^{3+} and TeO_2^{3+} peaks are observed, respectively. The peaks ranging from 20 to 30 μs [Fig. 2(b)] are identified as Te^+, TeO^+ and TeO_2^+ ions at 25.6 μs, 27.2 μs and 29 μs, respectively. Fig. 2(c) shows the 30–45 μs domain in which the heaviest species appear such as the singly charged Te dimer (Te_2^+), Te_2O^+, $Te_2O_2^+$, $Te_2O_3^+$, $Te_2O_4^+$ and the singly charged Te trimer (Te_3^+) between 36 and 45 μs.

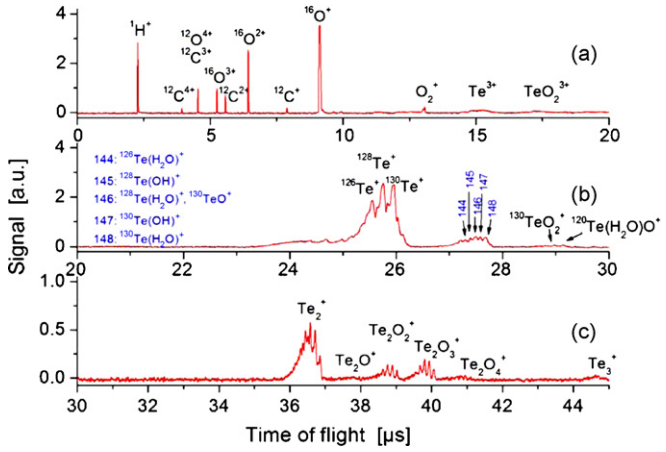

Fig. 2. Typical TOFMS spectra of the TeO_2 using a single-pulse fs irradiation in the range: (a) 1–20 μs, (b) 20–30 μs and (c) 30–45 μs. The pulse energy of the femtosecond laser was 3.0 μJ/pulse (fluence 1.0 J cm^{-2}, peak intensity 6.4×10^{12} W cm^{-2}).

Fig. 3 presents a close up of the Te monomer and dimer peaks when using 2.1 μJ/pulse energy (fluence 0.7 J cm^{-2}, peak intensity 4.5×10^{12} W cm^{-2}). The high-resolution view of Te^+ peak ion reveals that 6 different isotopes (^{122}Te, ^{124}Te, ^{125}Te, ^{126}Te, ^{128}Te, ^{130}Te) are clearly present in the spectrum (Fig. 3(b)). Tellurium has eight natural isotopes of which six are recognizable in our spectrum. The other two peaks are not visible due to the low relative quantity ratio. The close up of the Te_2^+ peak shows the combinations of the isotopes. Taking into account the probability of the different Te isotopes (taken from Ref. [16]), the peaks are assigned as shown in Fig. 3(c).

3.1.1. *Influence of the fs pulse energy on the species produced during fs-laser ablation*

Increasing the fs-laser pulse energy can give rise to the formation of new peaks and species in the spectrum as demonstrated in Fig. 4. The laser pulse energy was systematically increased until the first ion signals appeared. Below 0.7 μJ/pulse (fluence 0.2 J cm^{-2}, peak intensity 1.5×10^{12} W cm^{-2}) no relevant signal was detected. The first TeO_2 ablation related ion signals appear at a threshold pulse energy of 0.7 μJ/pulse. The signal can be observed at

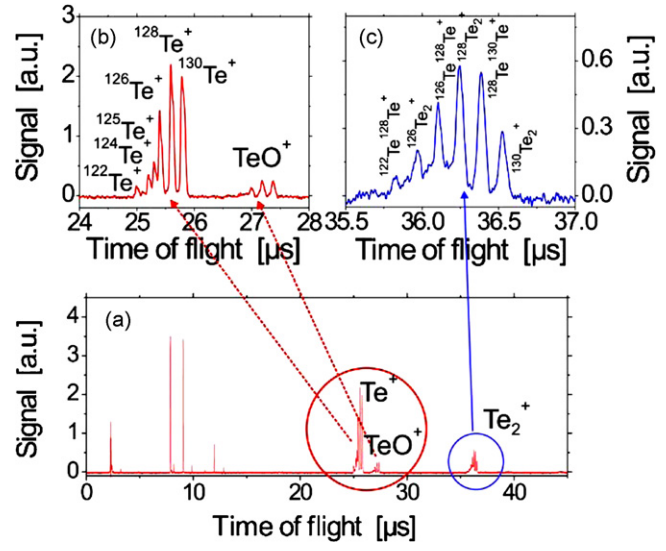

Fig. 3. Close up of the Te monomer and dimer peaks in the TOFMS spectrum indicating the presence of several isotopes in the ablation plume (fs pulse energy 2.1 μJ, fluence 0.7 J cm^{-2}, peak intensity 4.5×10^{12} W cm^{-2}).

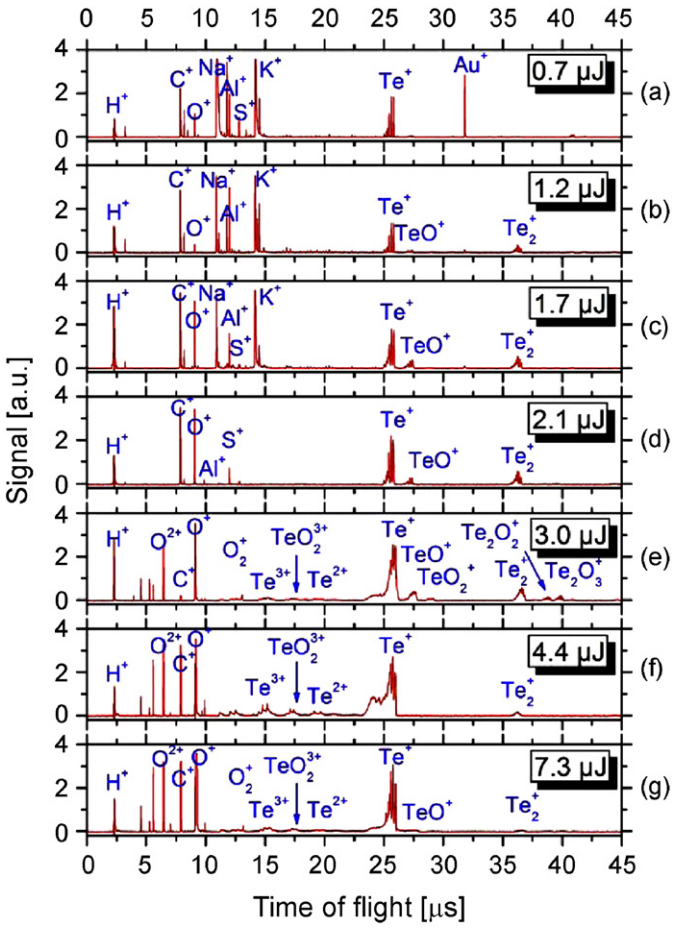

Fig. 4. TOFMS of c-TeO_2 using a single-pulse fs irradiation in the TOFMS range 1–45 μs. The pulse energy was changed from 0.7 to 7.3 μJ/pulse.

~25.6 μs and it is associated with the detection of Te^+ [Fig. 4(a)]. The peak is broadened due to the presence of the different Te isotopes (as discussed in Section 3.1). From 1.2 μJ laser pulse energy (fluence 0.4 J cm^{-2}, peak intensity 2.6×10^{12} W cm^{-2}), the TeO^+ peak together with the Te dimer (Te_2^+) peak start to evolve at ~27.1 μs and ~36.5 μs [Fig. 4(b)–(g)]. The O^+ peak at 9.4 μs is present throughout the whole energy range indicating that singly ionized oxygen is always produced in the course of fs-laser ablation.

At 3 μJ laser pulse energy (fluence 1.0 J cm^{-2}, peak intensity 6.4×10^{12} W cm^{-2}), the $Te_2O_2^+$ and the $Te_2O_3^+$ peaks appear at ~38.9 μs and 39.8 μs, respectively [Fig. 4(e)]. Te trimer (Te_3^+) at 44.7 μs becomes visible [a higher magnification of this peak can be seen in Fig. 2(c)]. Up to 3 μJ/pulse, the amplitude of the Te dimer peak slightly increases, however at higher energies (above 3 μJ) it starts to decrease indicating that high laser pulse energies do not favor the Te dimer formation. TeO^+ peak also decreases with higher pulse energy.

Above 3 μJ pulse energy double and triple charged species (Te^{2+}, TeO_2^{3+}) are also observed, which can be explained by the high peak intensity. In case of fs-laser irradiation light elements are also observed in the spectra (in the 1–15 μs range) since fs pulse can disintegrate materials into atoms more efficiently than ns-laser pulses due to much higher peak intensity [17]. When low laser pulse energies were used (0.7–1.7 μJ), several different peaks of Na^+, Al^+, Si^+, S^+ and K^+ ions can be observed originating from contaminations on the surface. The Gold ions ($^{197}Au^+$) can be recognized at 32 μs as shown in Fig. 4(a) deriving from the gold thin films deposited on TeO_2 to avoid the electronic charging.

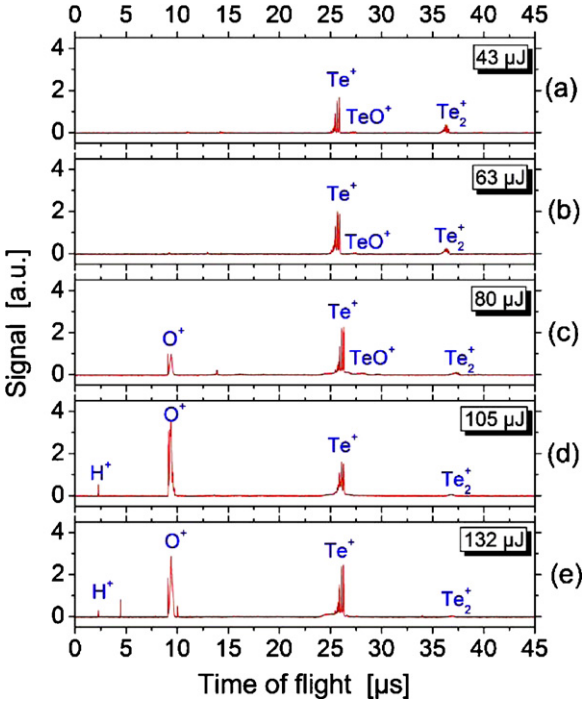

Fig. 5. TOFMS of c-TeO_2 using a single-pulse ns irradiation in the TOFMS range of 1–45 μs. The pulse energy was changed from 43 to 132 μJ/pulse.

Te^+ is produced by the dissociation of the Te dimer (Te_2^+) during its flight (metastable dissociation). The shifted time depends on the position where metastable dissociation takes place. The shoulder observed at around 24.5 μs in case of high pulse energies is associated with the distortion of the Te^+ peaks. This happens often when high laser energy is used. Along with this phenomenon, the mass resolution becomes worse as it can be observed in Fig. 4(e) and (f). The distortion is caused by the shielding of the acceleration voltage due to the high-density plasma induced by laser ablation. It does not appear for light ions such as H^+ and C^+ since they travel away quickly before the high-density part of the plasma cloud develops.

3.2. Nanosecond laser ablation

In case of ns-laser irradiation, the same method was used as in case of the fs irradiation to determine the threshold laser pulse energy. The results are shown in Fig. 5. The first ion signals were observed at a laser pulse energy of 43 μJ (fluence 14 J cm^{-2}, peak intensity 3.4×10^9 W cm^{-2}) [Fig. 5(a)]. It is interesting to note that there is almost no formation of TeO^+ and multiple charged species are observed in the course of ns ablation even at large pulse energy – in contrast to the fs ablation. The three-order difference in the peak intensity between the fs and ns-laser pulses seems crucial in the formation of these species.

Oxygen ions $^{16}O^+$ (9.3 μs) are produced for laser pulse energies exceeding 80 μJ (fluence 26.1 J cm^{-2}, peak intensity 6.4×10^9 W cm^{-2}) [see Fig. 5(c)–(e)]. The main species observed in the ns ablation are Te^+ and O^+. The signal of the singly charged Te dimer (Te_2^+) (37.2 μs) gradually decreases with increasing pulse energy. It disappears almost completely at 132 μJ (fluence 43 J cm^{-2}, peak intensity 10.5×10^9 W cm^{-2}) [Fig. 5(e)] indicating that high laser energy restrains the Te dimer formation. It is assumed here that high laser fluence disables the formation of Te dimer ions and only singly charged O^+ and Te^+ are produced as it was also observed in case of the fs irradiation.

The shoulder at around 24.5 μs is visible also in case of the ns ablation when the pulse energy is higher than 105 μJ (fluence 34.2 J cm^{-2}, peak intensity 8.4×10^9 W cm^{-2}), indicating that its origin does not depend on the laser pulse duration and the peak intensity, however it happens in both cases when using large pulse energy.

4. Conclusions

In this study single-pulse fs (pulse duration ~200 fs, wavelength 398 nm) and ns (pulse duration 4 ns, wavelength 355 nm) laser ablation of single-crystalline TeO_2 was carried out using a reflectron TOFMS.

Due to the three-order difference of the peak intensities of the ns and fs-laser pulses, significant differences were observed regarding the laser-induced species in the plasma plume. Singly charged positive Te ions in the form of six isotopes were detected predominantly in the ablation plume in case of both ns and fs-laser irradiations. In case of the ns-laser ablation the TeO^+ formation was negligible compared to the fs case and there was no Te trimer (Te_3^+) formation observed.

The Te ion peak intensities in the TOFMS strongly depended on the applied laser pulse energy. Low laser pulse energies favor the formation of Te dimer species, however continuously decreased when the energy was increased. Tellurium trimer species were also observed when femtosecond laser (3 μJ/pulse) was used. O^+ was usually detected as a byproduct of the ns and fs-laser ablation. This study also confirmed that fs-laser pulses could disintegrate materials into atoms more efficiently than ns-laser pulses due to the much higher peak intensity.

Acknowledgement

S. Beke is thankful for the financial support of the Japan Society for the Promotion of Science.

References

[1] N. Uchida, Y. Ochmachi, J. Appl. Phys. 40 (1969) 4692.
[2] Ochmachi, Uchida, Rev. Electr. Commun. Lab. 20 (1972) 529.
[3] S. Beke, K. Sugioka, K. Midorikawa, A. Peter, L. Nanai, J. Bonse, J. Phys. D: Appl. Phys. 43 (2010) 025401.
[4] S. Beke, K. Sugioka, K. Midorikawa, J. Bonse, Proc. SPIE 7584 (2010) 758415.
[5] F. Poitrasson, X. Mao, S.S. Mao, R. Freydier, R.E. Russo, Anal. Chem. 75 (2003) 6184.
[6] Y. Matsuo, T. Kobayashi, M. Kurata-Nishimura, T. Kato, T. Motobayashi, J. Kawai, Y. Hayashizaki, J. Phys.: Conf. 59 (2007) 555.
[7] R. Stoian, H. Varel, A. Rosenfeld, D. Ashkenasi, R. Kelly, E.E.B. Campbell, Appl. Surf. Sci. 165 (2000) 44.
[8] H. Varel, M. Wähmer, A. Rosenfeld, D. Ashkenasi, E.E.B. Campbell, Appl. Surf. Sci. 127–129 (1998) 128.
[9] T. Kobayashi, T. Kato, Y. Matsuo, M. Kurata-Nishimura, Y. Hayashizaki, J. Kawai, Appl. Phys. A 92 (2008) 777–780.
[10] T. Kobayashi, Y. Matsuo, M. Kurata-Nishimura, Y. Hayashizaki, J. Kawai, Appl. Surf. Sci. 255 (2009) 9652.
[11] T. Kobayashi, T. Kato, Y. Matsuo, M. Kurata-Nishimura, Y. Hayashizaki, J. Kawai, J. Chem. Phys. 127 (2007) 061101.
[12] T. Kobayashi, T. Kato, Y. Matsuo, M. Kurata-Nishimura, J. Kawai, Y. Hayashizaki, J. Chem. Phys. 126 (2007) 111101.
[13] F. Schmidt, R. Voszka, Cryst. Res. Technol. 16 (1981) K127.
[14] Anderson Janotti, G. Chris, Van de Walle, Appl. Phys. Lett. 87 (2005) 122102.
[15] Guangming Li, Masayuki Nogami, Yoshihiro Abe, Phys. Rev. B 51 (1995) 14930.
[16] Chronological Scientific Tables 2006, Edited by National Astronomical Observatory, Maruzen Co. Ltd., 2005.
[17] M. Kurata-Nishimura, F. Tokanai, Y. Matsuo, T. Kobayashi, J. Kawai, H. Kumagai, K. Midorikawa, I. Tanihata, Y. Hayashizaki, Appl. Surf. Sci. 197–198 (2002) 715.